Seminar - 4. letnik

Landau levels in graphene

Author: Zala Lenarčič
Mentor: prof. Anton Ramšak

Ljubljana, December 2010

Abstract

In this seminar I present graphene, a new material with promising application possibilities and important fundamental physics aspects. Beside brief overview of its properties, I will concentrate on Landau levels - one of the phenomena that show extraordinary dependences due to graphene's unusual energy dispersion. I will derive Landau levels for standard electrons, for electrons in graphene and its bilayer and then compare them on the base of real experiment.

Contents

1 Introduction

Graphene is certainly a rising star in material science, which recently brought Nobel Prize to Andre Geim and Konstantin Novoselov for fabrication, identification and characterization of it. The reason why this was not done before the year of 2004 is in its structure. It is a 2D mono-atomic crystal, which are proven (Landau, Peierls) to be thermodynamically unstable. But the nature finds its own way, which is in the case of graphene such, that the 2D crystal becomes intrinsically stable by gentle crumpling in the third dimension[1]. Such 3D warping (observed on a lateral scale of 10nm) leads to a gain in elastic energy but suppresses thermal vibrations (anomalously large in 2D) which above a certain temperature can minimize the total free energy. Though, it still remained an experimental challenge to produce a single-atom layer. The awarded couple and their collaborators managed to overcome it by simple mechanical exfoliation method for extracting thin layers of graphite from a graphite crystal with Scotch tape and then transferred these layers to a silicon substrate. The problem is that graphene crystallites left on a substrate are extremely rare and hidden in a 'haystack' of thousands of thick graphite flakes. Therefore the critical ingredient for success was the observation that graphene becomes visible in a optical microscope if placed on the top of a Si wafer with a carefully chosen thickness of SiO_2, owing to a feeble interference-like contrast with respect to an empty wafer.

    This experimental discovery opened whole new area for testing graphene's extraordinary properties already theoretically predicted. Because of its unusual electronic energy dispersion, graphene has led to the emergence of concept of 'relativistic' particles in condensed-matter. In condensed-matter physics, the Schrödinger equation rules the world, usually being quite sufficient to describe electronic properties of materials. Graphene is an exception - its charge carriers mimic relativistic particles and are more easily and naturally described starting with the Dirac equation rather than the Schrödinger. The relativistic behavior of electron in graphene brought about new possibilities for testing relativistic phenomena, some of which are unobservable in high-energy physics. Among the most spectacular phenomena reported so far are the new quantum Hall effects [2] and minimum quantum conductivity in the limit of vanishing concentration of charge carriers[3]. Other

QED effects that cannot be tested in particle physics, but could be in graphene are also gedanken Klein paradox[4] (process of perfect tunneling of relativistic electrons through arbitrary high and wide barriers) and Zitterbewegung[5] (jittery movement of a relativistic electron due to interference between parts of its wavepacket belonging to positive and negative energy states).

One of the effects that change their form - comparing to the electrons described by Schrödinger equation - are also Landau levels. These are quantized energy levels for electrons in a magnetic field. They still appear also for relativistic electrons, just their dependence on field and quantization parameter is different. In this seminar, I will concentrate specifically on this aspect of graphene - I will derive the Landau levels for graphene (mono-layer) and briefly mention the results for the bilayer. At the end I will show also some experimental evidence that prove the theoretically predicted dependences.

2   Graphene's properties

Graphene is a single 2D layer of carbon, packed in a heksagonal (honeycomb) lattice, with a carbon distance of 0.142 nm. Some of its characteristics are [6]:

- density: the unit hexagonal cell of graphene contains two carbon atoms and has an area of 0.052 nm^2. We can thus calculate its density as being 0.77 mg/m^2. A hypothetical hammock measuring 1m^2 made from graphene would thus weight 0.77mg.

- optical transparency: It is almost transparent, since it absorbs $\pi\alpha \sim 2.3\%$ (where α is fine structure constant) of the light intensity, independent of the wavelength in the optical domain.

- strength: it has a breaking strength of 42N/m, which is 100 times more than that of the strongest hypothetical steel film of the same thickness. It should thus be possible to make an almost invisible hammock out of graphene and if it was 1 m^2 large it would hold approximately 4 kg heavy burden (cat), though its own weight would be less than a mg (cat's whisker).

- thermal conductivity: the thermal conductivity is dominated by phonons and has been measured to be approximately 5000 W/mK which is 10 times better than that of copper.

- electron mobility: graphene shows exceptional electronic quality. In a pronounced ambipolar electric field charge carriers can be tuned continuously between electrons and holes in concentration n as high as 10^{13}cm^{-2} and their mobilities μ can exceed 15000cm^{2}V^{-1}s^{-1} even under ambient conditions.

3   Energy dispersion

Many of graphene's properties have origins in its energy dispersion. Therefore it is worth calculating it. As mentioned, graphene is a 2D crystal with hexagonal structure consisting of a bipartite lattice of two triangular sublattices (because each unit cell contains two carbon atoms) (figure 1). Each atom is tied to its three nearest neighbors via strong σ bonds that lie in the graphene plane with angles of 120°. The forth valence electron is in the 2p$_z$ orbital that is orthogonal to the graphene plane. With such picture we can explain also crystal structure of graphite, which consists of layers of graphene, with strong intralayer coupling and weak interlayer binding. The weak interlayer coupling supposedly arises due to van der Waals interaction and the particular bonding mechanism along the
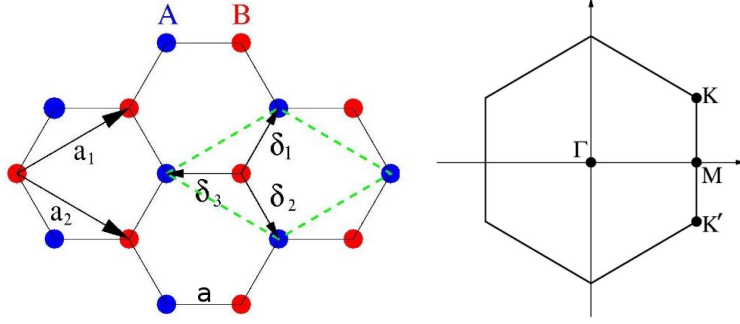
Figure 1: left: Bravais lattice with primitive vectors a_1, a_2 (a=0.142nm) and marked sublattices A and B, right: first Brillouin zone with marked corners K,K' of different symmetry

direction normal to the plane. Consequently, the separation between the adjacent layers (0.34nm) is much larger than the nearest neighbor distance between two carbon atoms (0.142nm). Similarly, carbon nanotubes and fullerenes can be formed.

I will give just a short description of its band structure, where I will neglect the corrugation of graphene. As shown on figure 1 let us name the primitive vectors in real space as $\mathbf{a_1}$ and $\mathbf{a_2}$ and in reciprocal lattice as $\mathbf{b_1}$ and $\mathbf{b_2}$. The real space lattice vectors and the corresponding reciprocal ones are

$$\mathbf{a_{1,2}} = \frac{\sqrt{3}a}{2}(\sqrt{3}, \pm 1), \quad \mathbf{b_{1,2}} = \frac{2\pi}{\sqrt{3}a}\left(\frac{1}{\sqrt{3}}, \pm 1\right)$$

where a=0.142nm is the distance between atoms.

The first Brillouin zone is a hexagon, where the corners form two inequivalent groups of K points, traditionally labelled K and K'

$$\mathbf{K} = \frac{2\pi}{3a}(1, \frac{1}{\sqrt{3}}), \quad K' = \frac{2\pi}{3a}(1, -\frac{1}{\sqrt{3}})$$

We will try to find the energy dispersion using tight binding approximation. For the wave function of graphene Ψ we take a linear combination of Bloch functions $\Phi_{n,\alpha}$ for sublattices A and B

$$\Psi(\mathbf{k}, \mathbf{r}) = \sum_{n,\alpha=A,B} c_{n,\alpha}(\mathbf{k})\Phi_{n,\alpha}(\mathbf{k}, \mathbf{r}), \quad \Phi_{n,\alpha}(\mathbf{k}, \mathbf{r}) = \frac{1}{\sqrt{N}}\sum_{\mathbf{R}} e^{-i\mathbf{k}\cdot\mathbf{R}}\phi_{n,\alpha}(\mathbf{r} - \mathbf{R})$$

Here N is the number of unit cells, $\mathbf{R}$ are the Bravais vectors that specify in which unit cell the atom is, $\phi_{n,\alpha}(\mathbf{r} - \mathbf{R})$ is orbital of the atom from the sublattice α, where n runs over all the four different orbitals of a carbon atom. With this ansatz we try to solve Schrödinger equation

$$(H_{at} + \Delta U)\Psi = \epsilon\Psi$$

where H_{at} is atomic Hamiltonian and ΔU is potential that comes from the interaction between atoms in crystal. If we solve this we get eight bands, corresponding to eight orbitals in a unit cell. We will concentrate only on the two $2p_z$ orbitals and their two bands. They are decoupled from the in-plane orbitals, since other orbitals and ΔU are all even in z and therefore all their integrals with ϕ_{p_z} vanish. By multiplying Schrödinger equation with $\langle\phi_{p_z,A}(\mathbf{r})|$ and $\langle\phi_{p_z,B}(\mathbf{r})|$ in the approximation

where we neglect nearest neighbor (and all the others) overlap $\langle\phi_{p_z,\alpha}(\mathbf{r}-\mathbf{R})|\phi_{p_z,\alpha'}(\mathbf{r}-\mathbf{R}')\rangle = 0$ if $R \neq R' \vee \alpha \neq \alpha'$ and include only nearest neighbor hoping $\langle\phi_{p_z,\alpha}(\mathbf{r}-\mathbf{R})|\Delta U|\phi_{p_z,\alpha'}(\mathbf{r}-\mathbf{R}')\rangle = t$, we get two equations for coefficients, which can be written in matrix form as

$$\begin{pmatrix} \epsilon_0 & t\,g(\mathbf{k}) \\ t\,g(\mathbf{k})^* & \epsilon_0 \end{pmatrix} \begin{pmatrix} c_A \\ c_B \end{pmatrix} = \epsilon \begin{pmatrix} c_A \\ c_B \end{pmatrix} \tag{1}$$

where $g(\mathbf{k}) = (1 + e^{-i\mathbf{k}\cdot\mathbf{a}_1} + e^{-i\mathbf{k}\cdot\mathbf{a}_2})$ and $\epsilon_0 = \langle\phi_{p_z,\alpha}(\mathbf{r})|H_{at}|\phi_{p_z,\alpha}(\mathbf{r})\rangle$. Taking into account the 3D warping, the nearest neighbor hoping parameters t are not equal, since orbitals are not parallel any more [7]. But this is beyond our scope. For the sake of further discussion, let us denote this system of equation a form of Hamiltonian H, being applied to the wave function $\psi = (c_A, c_B)^T$, $H\psi = \epsilon\psi$.

Setting $\epsilon_0 = 0$, the dispersion relation that we get from the determinant of the system (1) is

$$\epsilon(k_x, k_y) = \pm t\sqrt{1 + 4\cos\frac{3k_x a}{2}\cos\frac{\sqrt{3}k_y a}{2} + 4\cos^2\frac{\sqrt{3}k_y a}{2}} \tag{2}$$

It is plotted in the figure 2. We obtain two bands which are degenerated at the K and K' points.
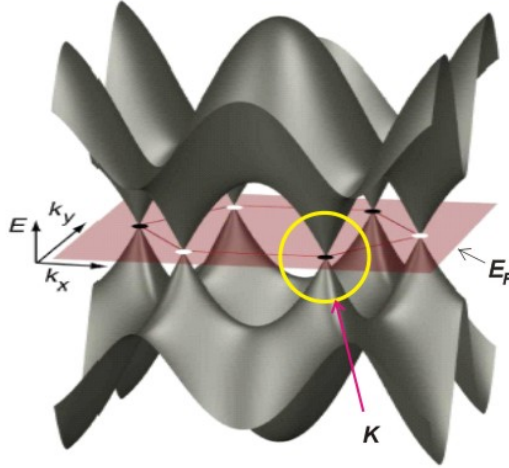

Figure 2: Energy dispersion with two band for the p_z electrons; red plane indicates the Fermi level, [8]

In an energy interval around these degeneration points, energy dispersion is characterizes by double cones. We will name the vicinity of K and K' points as valley K and valley K', respectively. What is more, the Fermi level of intrinsic graphene is situated at the connection points of this cones, because the two electrons from two atoms per unit cell just fill the lower band. Among the other six bands corresponding to in-plane orbitals, three of them lie below the p_z bands and the other three above. Of course, the lower ones are full and the upper empty. Since the density of states is zero at the points with Fermi energy, the electrical conductivity of intrinsic graphene is quite low.

The derivation of formula (2) neglected the overlap between next-nearest neighbors. Being included, they brings an asymmetry between electrons and holes (the two bands are not symmetrical any more).

4

3.1 Expansion around Fermi energy

The low-energy properties, corresponding to the electronic states near the Fermi energy, can be described by expanding the energy dispersion around the K and K' points. Let us write the graphene wave vector for valley K as $\mathbf{q} = \mathbf{K} + \mathbf{k}$. What we get for $|\mathbf{k}| \ll 1$ is

$$\epsilon(\mathbf{K} + \mathbf{k}) \approx \pm \hbar v_F |\mathbf{k}| \tag{3}$$

where $v_F = \frac{3a|t|}{2\hbar} \approx 10^6 m/s$ is Fermi velocity (which is comparable to that in metals). The expression for the expansion around K' is the same. The expression (3) corresponds to the two cones meeting at the K point with linear dependence on the wave vector. Because we know, that energy dispersion which is linear in wave vector belongs to massless particles, we say that electrons and holes with wave vectors close to K and K' points behave as massless. Those massless Dirac fermions made study of monolayer graphene so enticing.

As we know from particle physics, (almost) massless neutrinos are not described by Schrödinger equation, but by Dirac equation. Therefore, we would like to see whether Hamiltonian ascribed to our system (1) also have the form of Hamiltonian in the Dirac equation. Since particles behave as massless only around the K and K', we expand the Hamiltonian

$$H(\mathbf{q}) = \begin{pmatrix} \epsilon_0 & t\, g(\mathbf{q}) \\ t\, g(\mathbf{q})^* & \epsilon_0 \end{pmatrix}$$

around these points as well. The Hamiltonian in the vicinity of the K point is for $\mathbf{q} = \mathbf{K} + \mathbf{k}$

$$H_K^0(\mathbf{k}) = \hbar v_F \begin{pmatrix} 0 & i(k_x - ik_y) \\ -i(k_x + ik_y) & 0 \end{pmatrix} \tag{4}$$

which does not yet fully resemble the form of Dirac equation. To get rid of the imaginary factors, which spoil the equivalence, we redefine wave functions containing coefficients $c_{\alpha,\beta}$ as

$$\Psi_0^K = \begin{pmatrix} c_{A,K} \\ c_{B,K} \end{pmatrix} \to \Psi^K = \begin{pmatrix} -ic_{A,K} \\ c_{B,K} \end{pmatrix}, \quad \Psi_0^{K'} = \begin{pmatrix} c_{A,K'} \\ c_{B,K'} \end{pmatrix} \to \Psi^{K'} = \begin{pmatrix} c_{A,K'} \\ -ic_{B,K'} \end{pmatrix}$$

and consequently change the Hamiltonian, so that equations, coming from each line of the matrix representation of $H_K \Psi_K = \epsilon \Psi_K$, do not change. The new Hamiltonian is then

$$H_K(\mathbf{k}) = \hbar v_F \vec{\sigma} \cdot \mathbf{k} \tag{5}$$

where the $\vec{\sigma} = (\sigma_x, \sigma_y)$ is a vector of Pauli matrices. For the Hamiltonian in the vicinity of the K' holds $H_{K'}(\mathbf{k}) = -H_K^T(\mathbf{k})$. In relation with Dirac equation, we call the wave function Ψ^β spinor. In its upper and lower term it has the quantum mechanical amplitudes of finding the particle in one of the two sublattices A and B, respectively. And for each valley K and K' we have one such spinor. If we put them together in one bispinor $\Psi = (\Psi^{K'}, \Psi^K)^T$ and both Hamiltonian in a common one, we get

$$H\Psi = v_F \begin{pmatrix} -\vec{\sigma}^* \cdot \mathbf{p} & 0 \\ 0 & \vec{\sigma} \cdot \mathbf{p} \end{pmatrix} \Psi \tag{6}$$

Although we speak of Dirac particles, equation (6) is not completely the same as true Dirac equation which would be in chiral representation equal to

$$H\Psi = c \begin{pmatrix} -\vec{\sigma} \cdot \mathbf{p} & 0 \\ 0 & \vec{\sigma} \cdot \mathbf{p} \end{pmatrix} \Psi$$

It should be stressed, that Dirac equation in the case of graphene is a direct consequence of graphene's crystal symmetry. From the comparison we can see that k-independent Fermi velocity v_F plays the role of the speed of light. The role of spinor is transformed from storing the amplitudes for different spin projections to the amplitudes for different sublattices. Let us refer to this as to pseudospin. QED phenomena inversely proportional to the speed of light should be in graphene enhanced by a factor of $c/v_F \approx 300$ (e.g. fine structure constant which leaves consequences on enhanced interaction in many body physics). As we will see for the electrons in magnetic field pseudospin-related effects should generally dominate those due to the real spin.

4 Landau levels

4.1 Free electrons in a magnetic field

We will first investigate free electrons in a magnetic field, so that we can compare this to results obtained in a graphene layer. Let us orient the magnetic field in z-direction. The vector potential $\mathbf{A} = \nabla \times \mathbf{B}$ has only components perpendicular to $\mathbf{B}$. The whole Hamiltonian is given by [9]

$$H = \frac{1}{2m} \left(\hat{p}_{0x}^2 + \hat{p}_{0y}^2 + \hat{p}_z^2 \right), \quad \hat{p}_{0i} = \hat{p}_i - \frac{e}{c}\hat{A}_i \tag{7}$$

The third term in (7) corresponds to free motion in the z-direction, which can be separated off, since p_z commutes with first two terms. p_z contribution to the kinetic energy remains the same as for free particle. Let us work in Landau gauge, where $\mathbf{A} = (-By, 0, 0)$. In such a gauge $[H, p_x] = [H, p_z] = 0$, since Hamiltonian is not explicitly dependant on x and z. The eigenfunction will therefore have the form

$$\Psi(x, y, z) = e^{ik_z z} e^{ik_x x} \chi(y)$$

Let us find the energy eigenvalues E for stationary equation $E\Psi = H\Psi$, using that Ψ is eigenfunction of $\hat{p}_x$ and $\hat{p}_z$

$$H\Psi = \frac{1}{2m} \left((p_x + \frac{e}{c}B\hat{y})^2 + \hat{p}_y^2 + p_z^2 \right) \Psi$$

$$(E - E_z)\chi(y)e^{ik_z z}e^{ik_x x} = \left(\frac{1}{2}\frac{e_0^2 B^2}{mc^2}(\hat{y} - y_0)^2 + \frac{\hat{p}_y^2}{2m} \right) \chi(y)e^{ik_z z}e^{ik_x x}$$

The right-hand-side of the last equation has transparent form of Hamiltonian for harmonic oscillator, oscillating around $y_0 = \frac{p_x c}{eB}$. $\chi(y)$ will therefore be eigenfunction for such a 1D oscillator with eigenvalues equal to $\hbar\omega_c \left(n + \frac{1}{2} \right)$.

The energy levels for an electron in magnetic field are then

$$E_n = E_z + \hbar\omega_c \left(n + \frac{1}{2} \right), \quad \omega_c = \frac{e_0 B}{mc} \tag{8}$$

They are known as Landau levels. Since $E_n \neq E_n(k_x)$, they are very degenerated. Moreover, the wave functions corresponding to each level n are stationary. If we form a wavepacket out of different degenerated wave functions

$$\Phi(x, y, 0) = \int dk_x \, a_{k_x} e^{ik_x x} \chi_{k_x, n}(y) \rightarrow \Phi(x, y, t) = e^{-i\omega_c t(n+\frac{1}{2})} \int dk_x \, a_{k_x} e^{ik_x x} \chi_{k_x, n}(y)$$

its probability density will stay the same all the time. However, it will not feature classically expected circular motion.

Trying to pursue the analogy with classical picture, we calculate time dependence of coordinate operator $\hat{x}(t)$ (see [9])

$$x(t) = X - \frac{1}{\omega_c}\tau e^{-\omega_c \tau t}\dot{x}(0)$$

where

$$x \equiv \begin{pmatrix} x_1 \\ x_2 \end{pmatrix}, \quad X \equiv \begin{pmatrix} X_1 \\ X_2 \end{pmatrix}, \quad \tau = \begin{pmatrix} 0 & 1 \\ -1 & 0 \end{pmatrix}$$

for which $[X_1, X_2] = \frac{i\hbar}{m\omega_c}$. In classical mechanics, X would be the center of the circular orbits, since [9]

$$(x - X)^2 = \left(\frac{\tau e^{-\omega_c \tau t}\dot{x}(0)}{\omega_c}\right)^2 = \frac{\dot{x}^2(0)}{\omega_c^2} = const$$

However, in quantum mechanics wave function ψ describing the electron in magnetic field cannot be eigenfunction of X_1 and X_2 at the same time. Therefore the center of the orbit cannot be determined with arbitrary precision even in principle. Classical circular orbits can be (to certain precision) obtained only as a wave packet from the wave functions corresponding to different Landau levels.

Such derivation of Landau levels is appropriate also for electrons inside a material, as long as they come from parabolic energy bands with energy-momentum dispersion $E = E_\pm^0 \pm \hbar^2 k^2/2m^*$. The only difference is in m^* which is for such electrons effective mass with additional weight arising from interaction with the crystal lattice.

4.2   Landau energy levels in graphene

Similarly, the motion of relativistic charges in graphene in a strong magnetic field is also quantized. In a conventional electron gas (non-relativistic) Landau quantization produces equidistant energy levels, which is due to the parabolic dispersion law of free electrons. In graphene the electrons have relativistic dispersion law, which strongly modifies the Landau quantization of the energy and the position of the levels.

As for free electrons, we make the substitution $p_i \to p_{0i} = p_i - \frac{e}{c}A_i$. The Hamiltonian (6) will therefore change to

$$H = v_F \begin{pmatrix} 0 & -(p_{0x} + ip_{0y}) & 0 & 0 \\ -(p_{0x} - ip_{0y}) & 0 & 0 & 0 \\ 0 & 0 & 0 & p_{0x} - ip_{0y} \\ 0 & 0 & p_{0x} + ip_{0y} & 0 \end{pmatrix} \quad (9)$$

where the four-component wave function

$$\Psi = \begin{pmatrix} \Phi_A^{K'} \\ \Phi_B^{K'} \\ \Phi_A^K \\ \Phi_B^K \end{pmatrix}$$

corresponding to the Hamiltonian (9) now takes on broader meaning, such that Φ_A^K and Φ_B^K are envelope wave functions of A and B sites for the valley K, and $\Phi_A^{K'}, \Phi_B^{K'}$ for the valley K'.

7

For the magnetic field orthogonal to the graphene layer, the vector potential can be chosen in Landau gauge as $A = (-By, 0)$. For such gauge, $[H, \hat{p}_x] = 0$, p_x is good quantum number. Because equations for K and K' valley are decoupled, let us first look for the solutions of the K valley. We are solving the system

$$\begin{aligned} \epsilon \Phi_A^K &= v_F (\hat{p}_{0x} - i\hat{p}_{0y}) \Phi_B^K \\ \epsilon \Phi_B^K &= v_F (\hat{p}_{0x} + i\hat{p}_{0y}) \Phi_A^K \end{aligned}$$

which can be by inserting one equation into another further decoupled into

$$\epsilon^2 \Phi_A^K = v_F^2 (p_{0x} - ip_{0y})(p_{0x} + ip_{0y})\Phi_A^K \tag{10}$$
$$\epsilon^2 \Phi_B^K = v_F^2 (p_{0x} + ip_{0y})(p_{0x} - ip_{0y})\Phi_B^K \tag{11}$$

Let us find the energy levels ϵ for the Φ_B^K, using $[H, \hat{p}_x] = 0$ and that for electron $e = -e_0$

$$\begin{aligned} \frac{\epsilon^2}{v_F^2} \Phi_B^K &= \left(\left((\hat{p}_x + \frac{e}{c} B\hat{y}) + i\hat{p}_y \right) \left((\hat{p}_x + \frac{e}{c} B\hat{y}) - i\hat{p}_y \right) \Phi_B^K \right. \\ &= \left((\hat{p}_x + \frac{eB}{c}\hat{y})^2 - i \left[\hat{p}_x + \frac{eB}{c}\hat{y}, \hat{p}_y \right] + \hat{p}_y^2 \right) \Phi_B^K \\ &= \left((p_x + \frac{eB}{c}\hat{y})^2 + \frac{\hbar eB}{c} + \hat{p}_y^2 \right) \Phi_B^K \end{aligned}$$
$$\frac{1}{2m} \left(\frac{\epsilon^2}{v_F^2} + \frac{\hbar e_0 B}{c} \right) \Phi_B^K = \left(\frac{\tilde{k}}{2} (\hat{y} - y_0)^2 + \frac{\hat{p}_y^2}{2m} \right) \Phi_B^K$$

Where $\tilde{k} = \frac{e_0 B}{c\sqrt{m}}$, $y_0 = \frac{p_x c}{e_0 B}$. Again the right side of the equation has the form of Hamiltonian for the harmonic oscillator, oscillating around y_0. If Φ_B^K is eigenfunction of such Hamiltonian, its eigenvalues will be $\hbar \omega_c (n + \frac{1}{2})$ where as for the standard Landau quantization $\omega_c = \sqrt{\frac{\tilde{k}}{m}} = \frac{e_0 B}{mc}$. Consequently, the energy values for Landau levels in graphene monolayer must satisfy

$$\frac{\epsilon^2}{v_F^2} = \frac{\hbar e_0 B}{c}(2n + 1 - 1) \tag{12}$$

where $n = 0, 1, 2...$ goes through the same values as for harmonic oscillator. Since ϵ has positive and negative roots, we can extend the domain of n to integer values and write energy levels as

$$\epsilon = \text{sgn}(n)\sqrt{\frac{2\hbar e_0 B}{c}} v_F \sqrt{|n|} = \hbar \omega^{Dirac} \text{sgn}(n)\sqrt{|n|}, \quad \omega^{Dirac} = v_F \sqrt{\frac{2e_0 B}{\hbar c}} \tag{13}$$

The Landau level index, n, can be positive or negative. The positive values correspond to electrons (conduction band), while the negative values correspond to holes (valence band). Furthermore, they are not equidistant as in conventional case and the largest energy separation is between the zero and the first Landau level. This large gap allows one to observe the quantum Hall effect in graphene, even at room temperature [10].

In the above derivation we disregarded the spin of the electron, which brings additional twofold degeneracy of the Landau levels due to the spin. Because we are working with electrons in magnetic field, this degeneracy is actually splitted by the Zeeman interaction. Having derived the energy

difference between successive Landau levels, we can compare it to the strength of Zeeman interaction. For $B = 10T$, ratio between the latter and the difference between n=1,0 Landau level is

$$\frac{\hbar\omega_c/2}{v_F\sqrt{e\hbar B/c}} \approx 0.01$$

which in a way justifies our assumption for spin degeneration.

If we repeat the whole procedure also for equation (10) with Φ_A^K, we get

$$\frac{\epsilon^2}{v_F^2} = \frac{\hbar e_0 B}{c} 2(n+1), \quad n = 0, 1, ...$$

which, comparing to the previous result for Φ_B^K, lacks the level with $\epsilon = 0$. In terms of the occupation of the sublattices A and B, we can therefore expect interesting properties. Specifically, the wave function at the Landau level $n \neq 0$ should always have non-zero amplitudes on both sublattices A and B, while the wave functions at the Landau level $n = 0$ should have non-zero amplitude only on one sublattice: B sublattice for valley K or A sublattice for valley K'. The asymmetry between A and B sublattice originates from asymmetry in positions of the nearest neighbors for atoms at A and B sublattice. This property of the wave functions for the Landau levels in graphene makes the $n = 0$ level very special for different magnetic applications of graphene.

The wave functions corresponding to the Landau levels (13) are labeled by three indices (n-Landau level index, k-wave vector along the x-axis, K,K'-valley of wave vectors) and are given by the following expressions[10]

$$\Psi_{n,k}^K = \frac{C_n}{\sqrt{L}} e^{-ikx} \begin{pmatrix} 0 \\ 0 \\ \text{sgn}(n)(-i)\phi_{|n|-1,k} \\ \phi_{|n|,k} \end{pmatrix} \tag{14}$$

for valley K and

$$\Psi_{n,k}^{K'} = \frac{C_n}{\sqrt{L}} e^{-ikx} \begin{pmatrix} \phi_{|n|,k} \\ \text{sgn}(n)(-i)\phi_{|n|-1,k} \\ 0 \\ 0 \end{pmatrix} \tag{15}$$

for valley K'. Here L^2 is the area of the system,

$$C_n(x) = \begin{cases} 1 & \text{for n=0,} \\ \frac{1}{\sqrt{2}} & \text{for } n \neq 0 \end{cases}, \quad \text{sgn}(n) = \begin{cases} 0 & \text{for n=0,} \\ \frac{n}{|n|} & \text{for } n \neq 0 \end{cases}$$

$$\phi_{n,k} \propto \exp\left(-\frac{1}{2}\frac{(y-kl_B^2)^2}{l_B^2}\right) H_n\left[\frac{(y-kl_B^2)}{l_B}\right]$$

where $l_B = \sqrt{\hbar/eB}$ is the magnetic length and $H_n(x)$ are Hermite polynomials. $\phi_{n,k}$ is the wave function for a non-relativistic electron at the nth Landau level. All in all, their structure is reasonable: they are obviously eigenfunction of $\hat{p}_x$, in the $n = 0$ level only one sublattice is occupied and $(-i)$ factor comes from the redefinition of coefficients c_α. Another consequence of different dependence of energy levels on index n ($\epsilon_A \propto \sqrt{|n|-1}, \epsilon_B \propto \sqrt{|n|}$) for sublattices A and B results also in different wave functions $\phi_{n,k}$ at both sites, which must differ in their index n for 1 to yield the same energy eigenvalue for both. Figure 3 shows the the profile of wave functions in the K valley along the y-axis for the sublattices A and B in magnetic field B=10T for the index n=3.
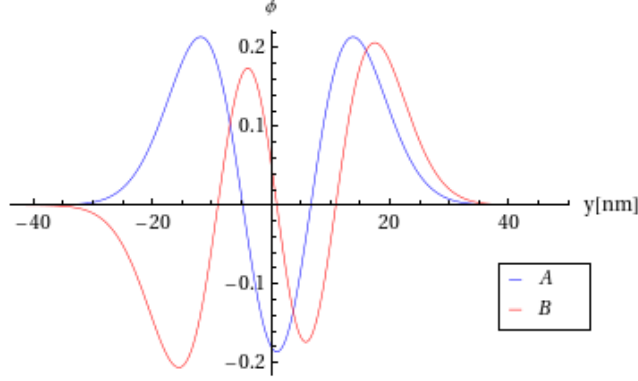
Figure 3: Profile of wave functions ϕ_n in the K valley along the y-axis on sublattices A (blue) and B (red) for n=3, $k = \frac{1}{100}K_x$ in magnetic field B=10T

4.3   Graphene bilayer

When two graphene layers stack to form a bilayer, the interlayer coupling leads to the appearance of band mass but it does not open a gap at the Dirac points. Here the Landau level spectrum takes the form

$$E_n = \text{sgn}(n)\hbar\omega_c\sqrt{|n|(|n|-1)}, \quad n \in Z, \quad \omega_c = \frac{eB}{m^*c} \tag{16}$$

This sequence is linear in field, similar to the standard case, but it contains an additional zero-energy level, which is independent of the field.

5   Experimental evidence

Experimentally, the Landau levels in graphene have been observed my measuring cyclotron resonances of the electrons and holes in infrared spectroscopy experiments[11] and by measuring tunneling current in scanning tunneling spectroscopy experiments [12].

In infrared spectroscopy experiments the Landau level optical transitions were studied. As we can expect from the theoretical derivation, the frequencies of all optical transitions in non-relativistic system are equal to the cyclotron frequency. On the other hand, since the Landau levels in graphene are not equidistant, all frequencies of optical transitions in graphene are different from each other. The cyclotron optical transitions in a graphene system are of two types: (i) intraband, i.e. transitions between the electron (hole) states; (ii) interband, i.e. transitions between the electron and hole states (conduction and valence bands).

In scanning tunneling spectroscopy experiments, the Landau levels are directly observed as the pronounced peaks in the tunneling spectra. From the positions of these peaks the energies of the Landau levels are directly extracted. Scanning tunneling spectroscopy enables selection of specific energy levels by varying the voltage bias between sample and tip, and the tunnelling current gives direct access to the density of states. Obtaining tunnelling spectra on graphene films is challenging because the films are quite small, and locating them in the field of view of a microscope can be daunting. As an example of such experiment confirmation, I will show the results reported in [12].

10

They worked on bulk samples of graphite, but surprisingly still managed to find massless and massive Dirac fermions, originating from mono- and bi-layers of graphene. This suggested decoupling of the surface state from the bulk.

An example of spectra measured on the surface of graphite at 4.4K in magnetic field up to 12T shows figure 4 (left). We can see, that all peaks except the two labelled A and Z, shift away
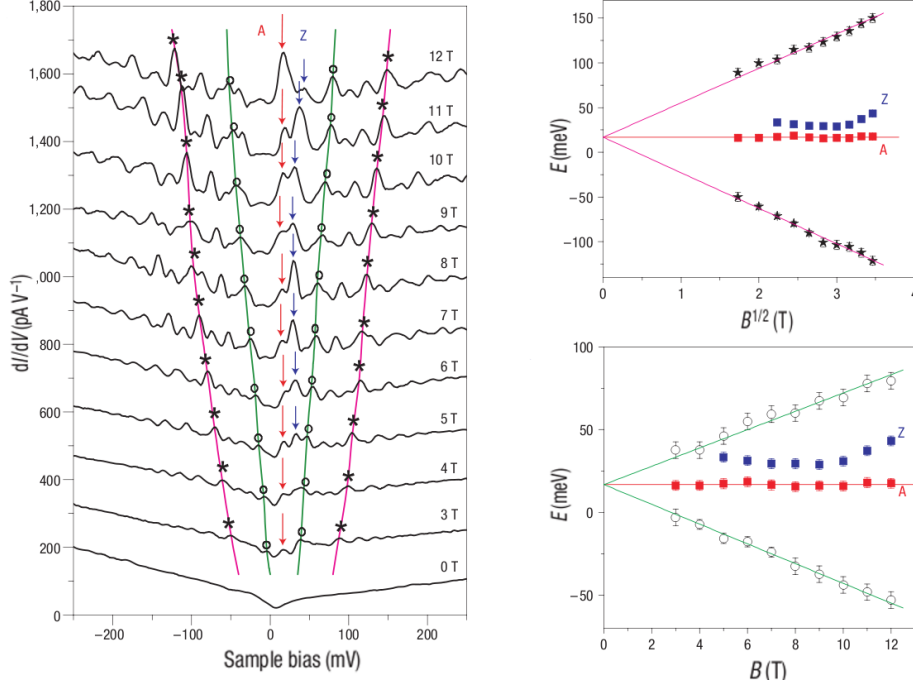

Figure 4: left: magnetic-field dependence of tunneling spectra on graphite surface at 4.4K. The spectra are shifted vertically by 150pAV^{-1} for clarity. right-up: Field dependence for Landau levels (LL) marked with stars. right-down: Field dependence for LL marked with circles. Figure reproduced from Ref. [12]

from the origin with increasing field. Peak A is independent of field, whereas peak Z shows weak non-monotonic field dependence associated with the n=0,-1 bulk Landau levels of graphite [13]. Analyzing the field dependence of the spectra, we find two families of peaks: one with square-root dependence and the other linear. The peaks marked with stars are members of the first family. Their square-root field dependence becomes more evident if we plot the peaks positions against $\sqrt{B}$ (figure 4 right,up). Positive energy sequence with positive slope corresponds to electron-like excitations, whereas the negative energy sequence with negative slope indicates hole-like behavior. The fact that both sequences extrapolate to the same field value implies that the conductance and valence band touch. What is more, the intersection point coincides with field independent peak A. Comparison with equation (13) suggests that the square-root sequence corresponds to the Landau levels of massless fermions, in which case we need to include peak A and identify its energy with K and K' points energy.

The peaks marked with circles are members of the family with linear field dependence. If we plot their positions against B (fig. 4 left, down), we again get the sequence with positive (negative)

energy which is also attributed to electron-like (hole-like) excitations. Here as well, both sequences extrapolate to the same energy at zero field, indicating that the conduction and valence band touch. The linear field dependence implies finite mass, but whether it represents standard particles (as free, but with effective mass) or electrons from graphene bilayer can be determined only by analysing the dependence on index n.

We proceed to analyze the dependence on n. To see which peaks (beside stared) also have square-root field dependence, we replot the spectra (fig. 4 left) against the scaled energy $E/\sqrt{B}$ with the energy origin shifted to the ϵ_0. It is now straightforward to identify a family of peaks that align on the same value of scaled energy. All the aligned peaks are then indexed starting with the n=0 level (peak A) at the origin. When we plot (fig. 5 right,down) the scaled energy of the aligned peaks against $\sqrt{|n|}$, the square-root dependence on level index becomes evident. From the latter, it is obvious that stared peaks do correspond to the electrons from the graphene monolayer, since also n dependence is the same as theoretically predicted.
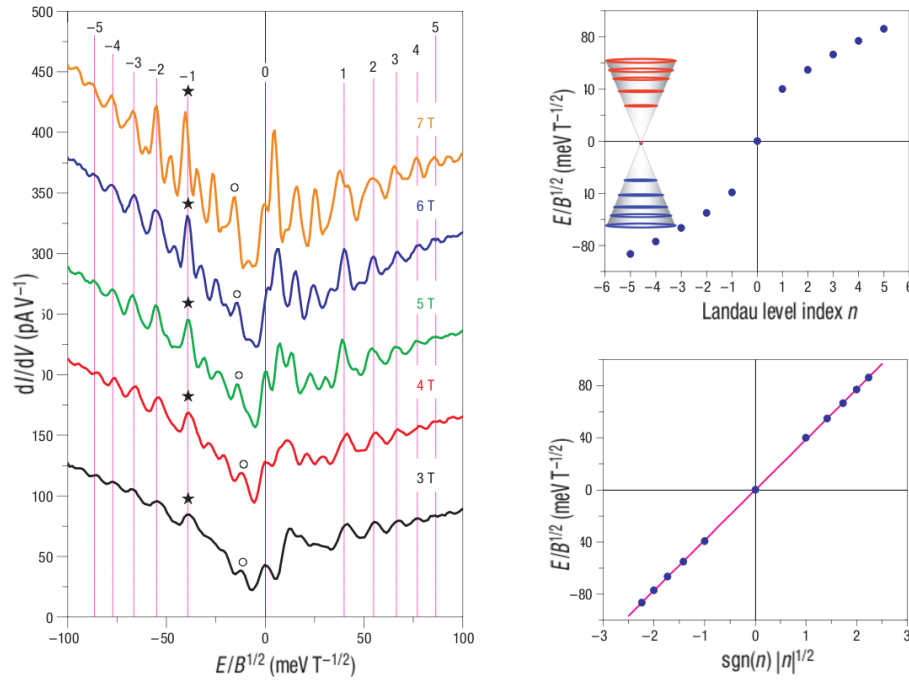

Figure 5: left: spectra against the scaled energy $E/B^{1/2}$ right-up: Landau levels peaks in units of $E/B^{1/2}$ against their index n. right-down: peaks in units of $E/B^{1/2}$ against $\mathrm{sgn}(n)\sqrt{|n|}$. Figure reproduced from Ref. [12]

To assign indexes to the peaks which show linear dependence on field, we replot the spectra against the scaled energy E/B. The question that we are mainly concerned with is whether those peaks correspond to standard particles or electrons from the bilayer of graphene. This question is directly connected to whether we should include in this family also the peaks labeled with A. If we leave them out and plot the other peaks against the index n (fig. 6 right-up), we get what should correspond to standard particles. But in this case two n=0 levels, marked with arrows are inexplicably missing. If we assume that spectrum corresponds to massive Dirac fermions from the
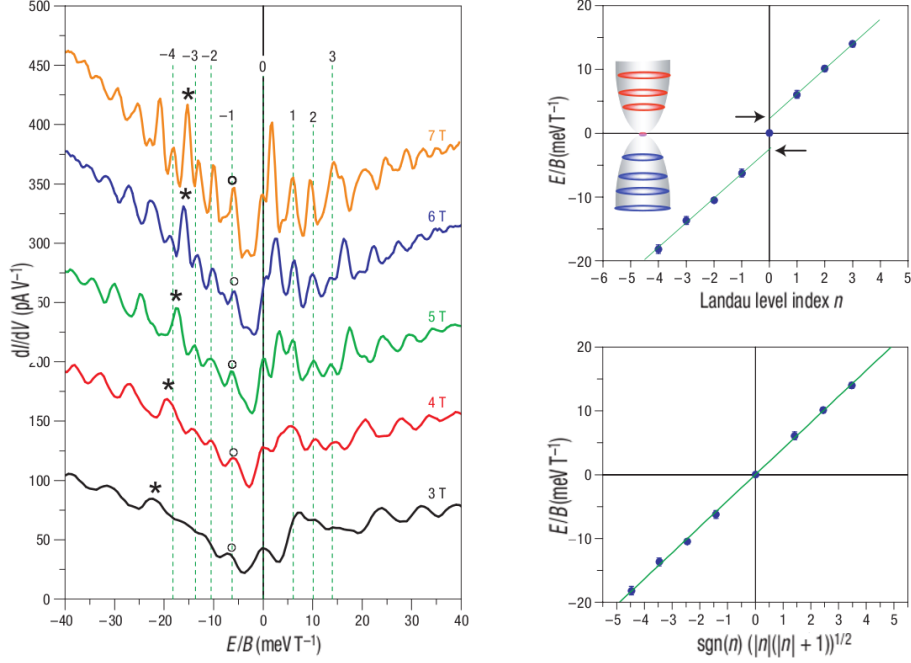
Figure 6: left: spectra against the scaled energy E/B right-up: Landau levels peaks in units of E/B against their index n. right-down: peaks in units of E/B against $\mathrm{sgn}(n)\sqrt{|n|(|n|+1)}$. Figure reproduced from Ref. [12]

graphene bilayer, then peak A should be included as the n=0 level and the other aligned peaks are labelled in ascending order as shown in fig. 6 left. Plotting the scaled energy for this sequence against $\sqrt{(|n|(|n|+1))}$ in fig. 6 (right-down), we now find agreement with equation (16) in support of the interpretation in terms of massive Dirac fermions. From the slope of these data we obtain an effective mass of $m^* = (0.028 \pm 0.003)m_e$ for both electrons and holes, where m_e is the free-electron mass. So their mass is still much smaller than the free one.

Data still has some unidentified peaks, but classification of this group requires detailed band-structure calculations.

The experiment reported shows strong indication of purely two-dimensional quasiparticles, although they were measured on bulk graphite, where their spectral weight should be negligible, compared to that of bulk excitations. The finding reported strongly suggest that only a few top layers of the graphite contribute to the observed electronic states. Since two-dimensional quasiparticles are not observed in the scanning tunnelling spectra in all types of graphite, material structure obviously plays an important role. Therefore more detailed theoretical modelling is needed to understand the scanning tunneling spectra and the two-dimensional nature of the quasiparticles in the surface of graphite.

6   Conclusion

Throughout the seminar, I have (partially) explained just one phenomena that mirrors graphene's extraordinary properties. To show its importance, I should stress that Landau levels are not just a lonely example, studied for the sake of fundamental knowledge, but are crucial ingredient for explanation of other graphene's features. One of those is quantum Hall effect, where the quantum conductivity σ_{xy} is shifted with respect to the standard QHE sequence by $1/2$, so that $\sigma_{xy} = \pm 4e^2/h(n + 1/2)$, where n is the Landau level index. The existence of a quantized level at zero energy, which is shared by electrons and holes is essentially everything one needs to know to explain the anomalous QHE sequence[10]. Similarly, with use of Landau levels in graphene bilayer, one can again explain QHE typical for this case. Moreover, because of the large energy difference between Landau levels with n=0 and n=1, the QHE in graphene can be observed at room temperatures[14].

Due to space limitations many other interesting topics were left unmentioned. To further motivate the research on these area, I will just name some of graphene's major potential applications. The use of graphene powder in electric batteries is because of its large surface-to-volume ratio and high conductivity expected to lead to improvements in the efficiency of batteries[15]. Because of weak spin-orbit coupling and the absence of hyperfine interaction it makes an excellent material for spin qubits. Furthermore, it has been suggested that graphene is capable of absorbing hydrogen since theoretical calculations predict that regular or irregular combinations of sp^3-bonded carbon atoms and graphene fragment are advantageous for molecular hydrogen storage. And it has been measured that the isosteric heat of adsorption indicates a favorable interaction between hydrogen and surface of the graphene sheets[16].

It is therefore justified to say that: although it should not exist - since it was found - it certainly is a material with promising future.

References

[1] J.C. Meyer, AK Geim, MI Katsnelson, KS Novoselov, TJ Booth, and S. Roth. The structure of suspended graphene sheets. *Nature*, 446(7131):60–63, 2007.

[2] Y. Zhang, Y.W. Tan, H.L. Stormer, and P. Kim. Experimental observation of the quantum Hall effect and Berry's phase in graphene. *Nature*, 438(7065):201–204, 2005.

[3] KS Novoselov, AK Geim, SV Morozov, D. Jiang, M.I.K.I.V. Grigorieva, SV Dubonos, and AA Firsov. Two-dimensional gas of massless Dirac fermions in graphene. *Nature*, 438(7065):197–200, 2005.

[4] MI Katsnelson, KS Novoselov, and AK Geim. Chiral tunnelling and the Klein paradox in graphene. *Nature Physics*, 2(9):620–625, 2006.

[5] MI Katsnelson. Zitterbewegung, chirality, and minimal conductivity in graphene. *The European Physical Journal B*, 51(2):157–160, 2006.

[6] The Royal Schwedish Academy of Science. Scentific Background on the Nobel Prize in Physics 2010. `http://nobelprize.org/nobel_prizes/physics/laureates/2010/sciback_phy_10_2.pdf`, 2010.

[7] MI Katsnelson and AK Geim. Electron scattering on microscopic corrugations in graphene. *Philosophical Transactions A*, 366(1863):195, 2008.

[8] http://www.ua.ac.be/main.aspx?c=ramezanimasir.massoud.

[9] Franz Schwabl. *Quantum Mechanics.* Springer, 4th edition, 11 2007.

[10] Y. Zheng and T. Ando. Hall conductivity of a two-dimensional graphite system. *Physical Review B*, 65(24):245420, 2002.

[11] RS Deacon, K.C. Chuang, RJ Nicholas, KS Novoselov, and AK Geim. Cyclotron resonance study of the electron and hole velocity in graphene monolayers. *Physical Review B*, 76(8):81406, 2007.

[12] G. Li and E.Y. Andrei. Observation of Landau levels of Dirac fermions in graphite. *Nature Physics*, 3(9):623–627, 2007.

[13] T. Matsui, H. Kambara, Y. Niimi, K. Tagami, M. Tsukada, and H. Fukuyama. STS observations of Landau levels at graphite surfaces. *Physical review letters*, 94(22):226403, 2005.

[14] KS Novoselov, Z. Jiang, Y. Zhang, SV Morozov, HL Stormer, U. Zeitler, JC Maan, GS Boebinger, P. Kim, and AK Geim. Room-temperature quantum Hall effect in graphene. *Science*, 315(5817):1379, 2007.

[15] S. Stankovich, D.A. Dikin, G.H.B. Dommett, K.M. Kohlhaas, E.J. Zimney, E.A. Stach, R.D. Piner, S.B.T. Nguyen, and R.S. Ruoff. Graphene-based composite materials. *Nature*, 442(7100):282–286, 2006.

[16] G. Srinivas, Y. Zhu, R. Piner, N. Skipper, M. Ellerby, and R. Ruoff. Synthesis of graphene-like nanosheets and their hydrogen adsorption capacity. *Carbon*, 48(3):630–635, 2010.